Zeitschrift: IABSE reports = Rapports AIPC = IVBH Berichte

Band: 41 (1983)

Artikel: Modelling of ship collisions against protected structures

Autor: Brink-Kjær, Ole / Brodersen, Finn Primdahl / Nielsen, Arne Hasle

DOI: https://doi.org/10.5169/seals-31660

Modelling of Ship Collisions against Protected Structures

Essais sur modèle de collisions de navires contre des structures de protection

Modellversuche für Schiffkollisionen gegen Schutzbauten

Ole BRINK-KJÆR
Senior Hydraulic Engineer
Danish Hydraulic Institute
Hørsholm, Denmark

Finn Primdahl BRODERSEN
Hydraulic Engineer
Danish Hydraulic Institute
Hørsholm, Denmark

Arne Hasle NIELSEN
Deputy Director
Danish Hydraulic Institute
Hørsholm, Denmark

Ole Brink-Kjær, born 1950, holds M.Sc. and Ph.D. degrees from the Technical University of Denmark. For six years he has been working within computational hydraulics, especially on storm surge and wave modelling. He has been responsible for the assessment of extreme environmental conditions for several offshore and coastal engineering projects.

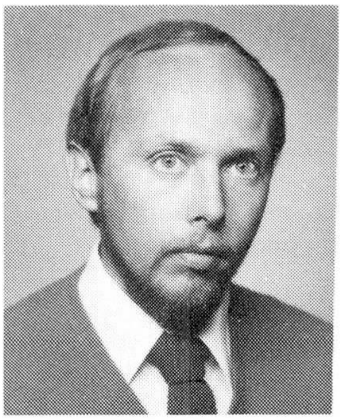

Finn Primdahl Brodersen, born 1950, got his M.Sc. in civil engineering at the Technical University of Denmark. For 4 years he was working with hydraulic models, mainly concerning breakwater stability and wave disturbance in harbours. Since 1979 he has been involved in the design and supervision of marine pipelines.

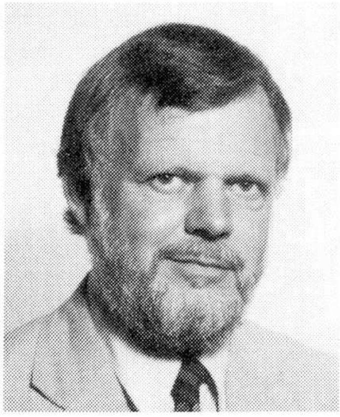

Arne Hasle Nielsen, born 1934, holds M.Sc.'s from the Technical University of Denmark (1958), and Berkeley University of California (1962) in Hydraulic and Marine Engineering. After a few years in consulting engineering, he joined DHI in 1964, where he has been in charge of numerous hydraulic studies in many countries.

SUMMARY

This paper describes how model tests and mathematical analysis techniques can be combined to reach a deterministic description of collisions between ships and protective structures, thereby providing an engineering tool which can be applied for the design of protective structures with optimal stopping and deflecting capabilities. Results obtained for the now postponed Great Belt Bridge (Denmark) illustrate the application of this technique for protective rubble mound structures.

RÉSUMÉ

Cet article décrit des essais sur modèle et des techniques d'analyse mathématique pour obtenir une description déterministe de collisions entre des navires et des structures de protection, procurant ainsi un moyen utilisable pour la conception et le projet de structures de protection ayant des capacités optimales d'arrêt et de déviation. Les résultats obtenus pour le "Great Belt Bridge" (Danemark), projet maintenant repoussé à une date ultérieure, illustrent l'application de cette technique aux structures de protection en enrochement.

ZUSAMMENFASSUNG

Dieser Artikel behandelt, wie Modellversuche und mathematische Analysetechnik vereint werden können, um Kollision zwischen Schiff und Schutzbauten zu beschreiben. Hiermit wird ein ingenieurmässiges Werkzeug gegeben, das für den Entwurf von Schutzkonstruktionen, mit optimalen stoppende und abweisenden Eigenschaften, geeignet ist. Resultate von der Grosse-Belt-Brücke, deren Bau jetzt verschoben ist, zeigen die Verwendbarkeit dieser Technik bei Steingeschützten Konstruktionen.

1. INTRODUCTION

The risks and the consequences of ship collisions are of govering importance for the design of many types of marine structures, such as bridge piers. Optimal design of protective structures requires a general understanding of the deflecting and stopping capabilities of such structures combined with methodologies for the accurate assessment of collision consequences as function of collision circumstances.

Model tests and mathematical analysis techniques can be important tools in the planning and design of protective structures by providing insight in the collision mechanism and the associated impact forces.

The empirical findings on ship collisions as they have been obtained from structural, soil mechanical and hydraulic model tests can be combined with a general mathematical formulation of the collision problem. This allows for a reliable extension of model test results to cover other conditions than those specifically tested. Such techniques were used to study protection islands for the planned Great Belt Bridge (Denmark) and results from these investigations are discussed in the present paper.

This paper describes collisions as function of:

- the speed, course, size, bow shape and hull stiffness of vessel
- the strength and geometrical shape of the protective structure.

The basic equations for the vessel's motion during collisions are presented in Chapter 2. A classical mechanical formulation, which takes into account all six degrees of freedom, is feasible and can be solved with only little computational effort. Basic information on the impact forces arising from the crushing of ship bows is outlined in Chapter 3. The following four chapters 4-7 deal with different combinations of the relative strength of the vessel and the protective structure, i.e. rigid - rigid, deformable - rigid, rigid - deformable and deformable - deformable.

A more detailed description is given in chapter 6 with rigid vessels against deformable protective structures, in this case rubble mound structures. This case is treated in detail because it demonstrates how findings from parallel studies within different engineering areas for a given project can be combined into one deterministic frame and verified against hydraulic model tests. Such tests were carried out for the planning of the now postponed, high level combined road- and railway bridge across the 15 km wide Great Belt (Denmark). Rubble mound structures around the bridge piers appeared to be a promising solution for protecting this bridge against ill-manouvred vessels passing along the main shipping route (20,000 vessels per year) from the North Sea to the Baltic countries. Fully loaded tankers up to 250,000 DWT may navigate in these waters. Existing information on collision between vessels and rubble mound slopes was found to be limited and not useful for design purposes. A series of studies were therefore initiated and interpretated as outlined in Chapter 6.

2. GENERAL FORMULATION OF EQUATIONS OF MOTION

The equations of the vessel's motion are most conveniently expressed by using two cartesian frames of reference:

1. A fixed cartesian frame of reference, Frame I, with horizontal x- and y-axes and a vertical z-axis.

2. A cartesian frame of reference, Frame A, which is fixed relative to the vessel. For this frame an index $_A$ is used. The origo is placed at the vessel's centre of gravity, and the x_A- and y_A-axis coincide with the vessel's longitudinal and transversal axis, respectively.

The translatory displacements of the vessel's centre of gravity are denoted x_G, y_G and z_G.

The angular displacements of the rotational motion around

firstly - the vertical axis through the vessel's centre of gravity.
secondly - the transversal axis of the vessel.
thirdly - the longitudinal axis of the vessel

are denoted RZ, RY and RX. The sequence of defining these angles is part of the definition. These angular movements are known as yaw, pitch and roll. For small values of the angular displacements, the translatory displacements x_G, y_G and z_G are known as surge, sway and heave.

The relationship between the coordinates of the two frames of reference becomes

$$\begin{bmatrix} x \\ y \\ z \end{bmatrix} = \begin{bmatrix} x_G \\ y_G \\ z_G \end{bmatrix} + \begin{bmatrix} C_{11} & C_{12} & C_{13} \\ C_{21} & C_{22} & C_{23} \\ C_{31} & C_{32} & C_{33} \end{bmatrix} \begin{bmatrix} x_A \\ y_A \\ z_A \end{bmatrix} \quad \text{,where}$$

$$\begin{aligned}
C_{11} &= \cos RY \cos RZ \\
C_{12} &= \sin RX \sin RY \cos RZ - \cos RX \sin RZ \\
C_{13} &= \cos RX \sin RY \cos RZ + \sin RX \sin RZ \\
C_{21} &= \cos RY \sin RZ \\
C_{22} &= \sin RX \sin RY \sin RZ + \cos RX \cos RZ \\
C_{23} &= \cos RX \sin RY \sin RZ - \sin RX \cos RZ \\
C_{31} &= -\sin RY \\
C_{32} &= \sin RX \cos RY \\
C_{33} &= \cos RX \cos RY
\end{aligned}$$

The next step is to express the accelerations $\ddot{x}_G, \ddot{y}_G, \ddot{z}_G, \ddot{RX}, \ddot{RY}$ and $\ddot{RZ}$ for given outer forces and moments as they may occur during a collision.

In order to facilitate a classical mechanical computational procedure, so-called added or hydrodynamic masses and moments of inertia are specified. In this manner it is taken into account that also the surrounding water undergoes accelerations whenever the vessel does.

For translatory movements in the direction of the x_A-axis it can be assumed that the acceleration will be equal to the outer force F_{xA} in the x_A-direction divided by the sum m_{xA} of the mass of the vessel and the added mass. Analogue assumptions are introduced for translatory movements in the direction of the y_A- and z_A-axis. Generally, m_{xA} is only a few per cent larger than the mass of the vessel whereas m_{yA} and m_{zA} can be twice the mass of the vessel. In the fixed frame of reference these equations can be written

$$\begin{bmatrix} F_x \\ F_y \\ F_z \end{bmatrix} = \begin{bmatrix} m_{11} & m_{12} & m_{13} \\ m_{21} & m_{22} & m_{23} \\ m_{31} & m_{32} & m_{33} \end{bmatrix} \begin{bmatrix} \ddot{x}_G \\ \ddot{y}_G \\ \ddot{z}_G \end{bmatrix}$$

where the non-diagonal elements generally are non-zero and only vanish for $RX = RY = RZ = 0$ (or $m_{xa} = m_{ya} = m_{za}$).

For rotational movements it can be assumed that the vessel's centre of the ellipsoid of inertia coincides with the vessel's centre of gravity and that the principal axes of the ellipsoid of inertia coincide with the x_A-, y_A- and z_A-axis. In analogy with the treatment of translatory movements, it is assumed that the angular acceleration around the x_A-axis is equal to the moment M_{xA} of the vessel's moment of inertia and the added moment of inertia. Analogue assumptions are introduced for angle accelerations around the y_A- and z_A-axis. If the generally valid vectorial moment equation is projected on the directions of the x_A-, y_A- and z_A-axis, the following equations are obtained

$$\begin{aligned} I_{xA}\,\dot{\Omega}_{xA} + (I_{zA} - I_{yA})\,\Omega_{yA}\,\Omega_{zA} &= M_{xA} \\ I_{yA}\,\dot{\Omega}_{yA} + (I_{xA} - I_{zA})\,\Omega_{zA}\,\Omega_{xA} &= M_{yA} \\ I_{zA}\,\dot{\Omega}_{zA} + (I_{yA} - I_{xA})\,\Omega_{xA}\,\Omega_{yA} &= M_{zA} \end{aligned}$$

where the angular velocity reads:

$$\begin{aligned} \Omega_{xA} &= \dot{RX} - \sin RY\,\dot{RZ} \\ \Omega_{yA} &= \cos RX\,\dot{RY} + \sin RX\,\cos RX\,\dot{RZ} \\ \Omega_{zA} &= \sin RX\,\dot{RY} + \cos RX\,\cos RY\,\dot{RZ} \end{aligned}$$

From these equations it is seen that $\ddot{RX}$, $\ddot{RY}$ and $\ddot{RZ}$ can be determined from $\dot{\Omega}_{xA}$, $\dot{\Omega}_{yA}$ and $\dot{\Omega}_{zA}$ which in turn can be determined from the outer moments.

As long as all outer forces and moments can be described as function of the vessel's instantaneous position (6 parameters) and velocity (6 parameters) - possibly with some knowledge of the prehistory such as deformations - the instantaneous accelerations can be found from the above described equations. Numerical integration can be carried out with only little computational effort and thereby provide the time history of a collision event of interest.

The added masses depend on frequency as described by Motora et al (1971). Rather than selecting a single representative value for given collision circumstances, the variation of the added masses and moment of inertia during the collision may be computed by a strip method where the forces acting on each section of the vessel are described by means of unit response functions, see Petersen (1980). Fig. No. 1 from this reference shows the ratios between the added mass (momentum of inertia) and the vessels's mass (momentum of inertia) for sway and yaw as function of cyclic frequency ω.

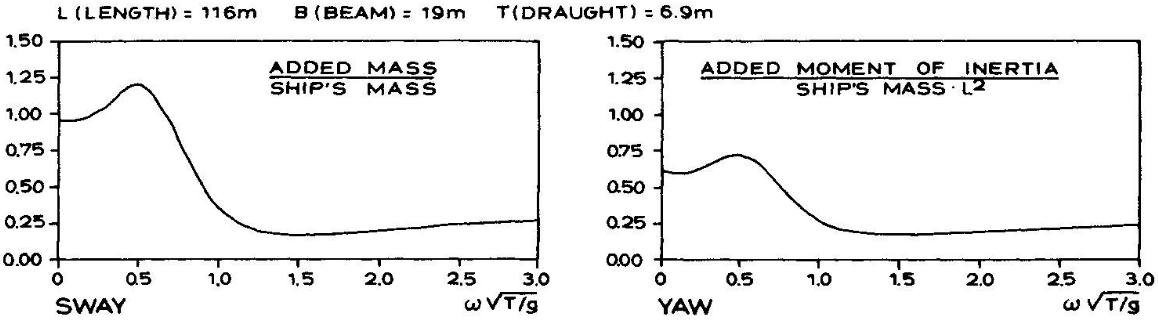

Fig. No. 1 Added Mass and Moment of Inertia for Sway and Yaw.

It is seen that these ratios are significantly larger for low-frequency disturbances - such as collisions between ships and structures - than they are for high-frequency disturbances. The proper assessment of these characteristics for sway and yaw is important when evaluating the deflecting characteristics of a protective structure and when evaluating the kinetic energy of a vessel drifting sideways (swaying) into a bridgepier or platform.

Following Salvesen (1970) hydrodynamic damping forces and moments can be assumed to be proportional to the six translatory and rotational velocities. Hydrodynamic restoring forces and moments can be assumed to be proportional to the displacement z_G, RX and RY; also a cross-coupling term between heave and pitch (z_G and RY) should be included.

The hydrodynamic damping forces are not of much importance for the evaluation of collision circumstances. The restoring forces play a more crucial role as they generally tend to bring the vessel back to a position with large contact forces and thereby transform the kinetic energy in a destructive manner with only little energy being transformed into potential energy expressed in terms of z_G, RX and RY.

3. COLLISION FORCES

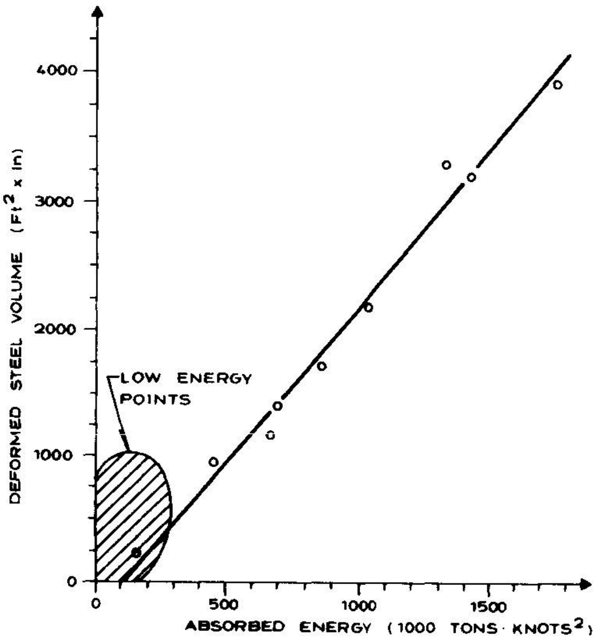

Fig. No. 2 Minorsky's Empirical Relationship between Impact Energy and Deformed Volume of Steel.

Minorsky (1959) derived a simple empirical relationship between absorbed energy and the volume of steel in the damaged portions of decks, longitudinal bulkheads and shell plating,see Fig. No. 2. For a given vessel an estimate of the load deformation curve can be reached from this relationship, e.g. as shown by Olnhausen (1966). Also, this simple relationship agrees surprisingly well with the experimental results of Woisin (1971) who rammed ship bows in scale 1:7.5 and 1:12 into strong protective structures for reactors in nuclear powered ships. Following Woisin, typical values of the average impact force to be reached during head-on collisions will range from 200-300-400 MN for 50-100-200 10^3 DWT vessels. In the very beginning of the collision, impact forces reaching twice these values may be experienced within short durations, say 0.1 sec. For a given size of vessel the impact force may deviate from the above typical figures by approx. 50 per cent.

Model results like those of Woisin (1971), Ando and Arita (1976), Arita et al (1977), Nagasawa el al (1977), and Iwai et al (1980) provide insight to the relationship between the load-penetration curve and the structures of the ship bow. In theoretical models the structures of the vessel can be decomposed into simpler structural elements. Reckling (1976,1977) obtained accurate agreement with Woisin's experiments by distinguishing between three major types of plastic damage : accordion-shaped folding of longitudinally stressed plating, tearing open of longitudinally stressed plating where the collision opponent intrudes, and tearing open of laterally stressed plating due to large membrane strains. Of special relevance for ship collisions against bridge piers is Reckling's calculation of the instability load of all the longitudinally stressed plating (decks) in a striking ship bow. The computed forces agreed within 10 to 20 per cent of the measured impact forces in the tests where the ship bow was completely damaged. Jones (1979) presents a litterature survey on these aspects of ship collisions.

4. RIGID VESSEL AGAINST RIGID STRUCTURE

The collision between a vessel and a sloping structure may as a first approximation be treated as a collision between two rigid bodies, the vessel responding to outer forces as outlined in Chapter 2. This is done by

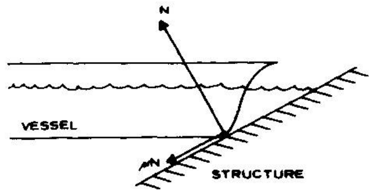

Fig No.3 Definition Sketch.

1) computing the impulses I (perpendicular to the slope) and μI (directed opposedly to the projected track on the slope of the vessel's collision point) which change the velocity of the vessel's collision point to become parallel to the slope.

2) computing the forces N and μN which accelerate the vessel in such a manner that the vessel's collision point remains at the slope (or ultimately loose contact).

The kinematic conditions from which the collision impulses and -forces are computed lead to simple linear equations which can be solved by standard methods. Computations of the entire collision providing time series of the collision force and the vessel's displacements and velocities can then be carried out for the full three-dimensional case as outlined in Chapter 2. The assumption of vessel and structure being rigid is only valid for some low-energy collisions or high-energy collisions with very small contact forces acting over long distances. However, the results which can be obtained with this assumption will provide upper- or lower-bound values for a number of parameters such as e.g. maximum potential energy in heave, roll and pitch (z_G,RX,RY) and maximum vertical displacement of vessel's bow. Such values can prove useful when evaluating the results and strategy of more detailed investigations.

5. DEFORMABLE VESSEL AGAINST RIGID STRUCTURE

If, in a collision scenario like that shown in Fig. No. 3, the sloping protective structure is a concrete structure with sufficient overall strength, the vessel will be the weaker part. In that case the simple kinematic condition of Chapter 4 has to be replaced by a load-penetration curve for the plastic deformation of the vessel.

Fuchs et al (1978) assumed the contact force to be proportional to the contact area with a velocity directed towards the sloping structure. The frictional force was computed as outlined in Chapter 4, μ=0.25 was applied. In order to keep track of the deformations, the vessel was sliced (computationally) in the longitudinal directions, and for each segment the individual contributions to the total outer force and moment were determined. The motions of the vessel were then determined in accordance with the theory presented in Chapter 2. Simulations were carried out for different combinations of vessel's speed, size, strength, angle of approch and for different slope angles.

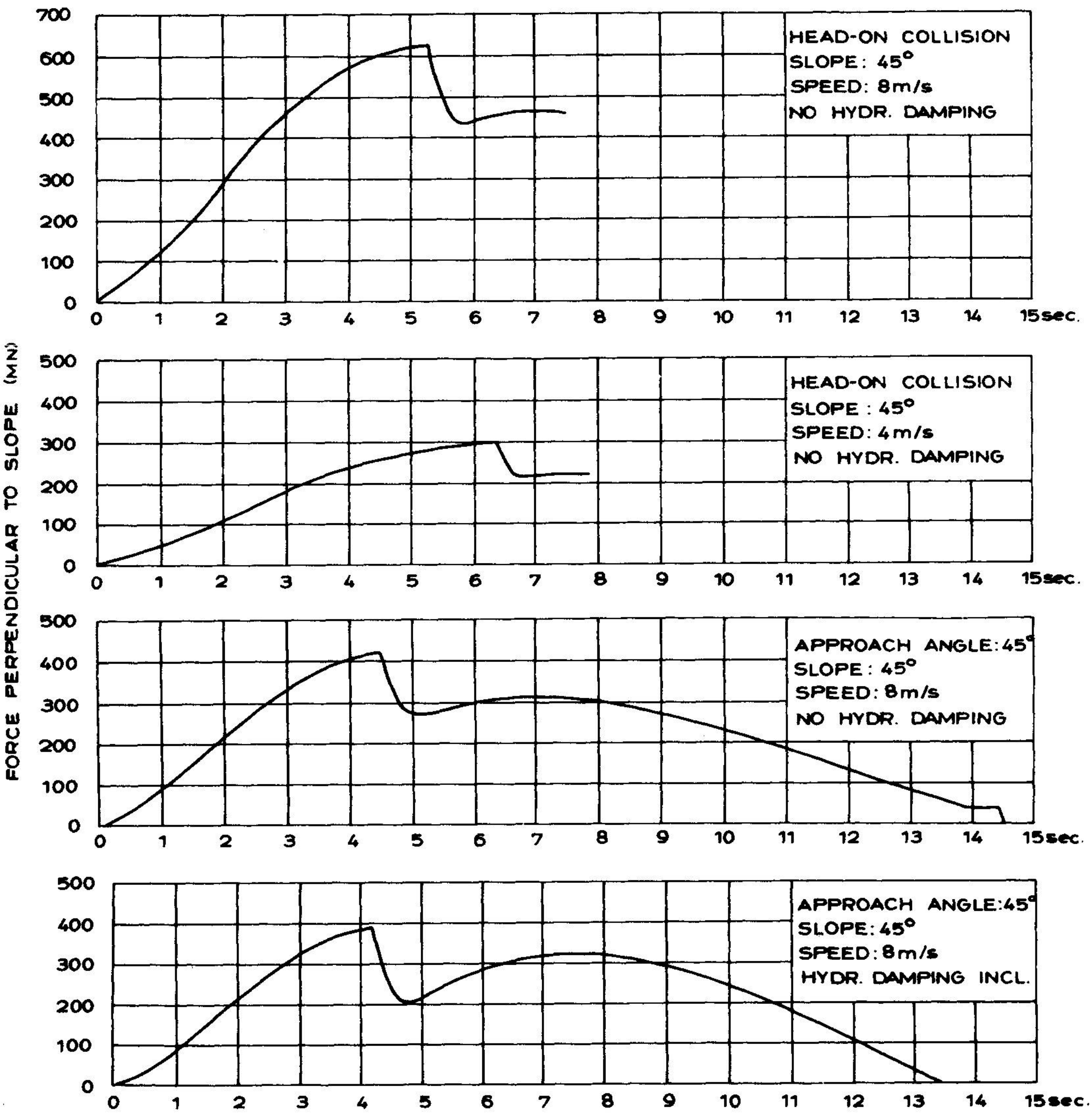

Fig. No. 4 Collision Forces for a fully Loaded 250,000 DWT Tanker Colliding with a Rigid Slope (1:1).

Fig. No. 4 shows four time series of the collision force perpendicular to the slope for a fully loaded 250,000 DWT tanker for which the contact-force area ratio in all cases is $4\ 10^5\ N/m^2$. The two upper time series refer to head-on collisions with initial vessel speeds of 8 m/s and 4 m/s, respectively. The two lower time series refer to obliquely incoming (45^o) vessels with an initial speed of 8 m/s and with hydrodynamic damping excluded and included, respectively.

For a slope angle of 45 degrees and a friction coefficient of 0.25, the horizontal force equals 88 per cent of the force perpendicular to the slope for head-on collisions. Except for this constant ratio the two upper curves show how the vessel's initial momentum (M_{xA} times initial vessel speed) is brought to zero by the time integrated horizontal force i.e.

$$m_{xA}\ V_{init} = \int F_{Horizontal}\ dt$$

The fastgoing vessel (upper curve) is more rapidly damaged and the maximum collision force, although appr. two times larger, is reached earlier than in the case for the more slowly moving vessel. The durations of these collisions events are almost identical.

For the obliquely incoming vessel, see the lower two curves of Fig. No. 4, the duration of the collision is considerable larger. This is so because of the large added mass and moment of inertia for sway and yaw. However, it is important to note that the maximum collision force is only appr. two-third of that experienced for the head-on collision with the same initial speed of vessel.

By comparing the two lower curves of Fig. No. 4 it is seen that the inclusion of the hydrodynamic damping terms are not of great significance.

6. RIGID VESSEL AGAINST DEFORMABLE STRUCTURE

In case the protective structure is a rubble mound structure, the vessel will be the stronger part - at least in the initial stages of a collision. In this chapter the collision characteristics of such protective structures will be discussed in rather detail. For the Great Belt Bridge Project, hydraulic model tests were carried out by the Danish Hydraulic Institute in order to provide insight to the dynamics of such collisions.

6.1 Study Program

A first series of tests was carried out for vessels colliding with an (infinitely) long rubble mound slope with a horizontal berm and a second series of tests were carried out for rubble mound islands with a horizontal berm. The purpose of the first series of tests was to provide insight to the stopping and deflecting capabilities of a rubble mound slope as function of

- shape of ship bow
- vessel's angle of approach
- speed of vessel
- vessel's size and load condition (draught)
- level of berm.

The purpose of the second series of tests was to test proposed configurations of protection island and thereby contribute to the design of protection islands with optimum deflecting and stopping capabilities.

The results of investigations in the areas of naval architecture and soil mechanics were applied in the formulation of a deterministic mathematical model following the theory outlined in Chapter 2. The purpose of developing such a model was to interrelate the results of hydraulic and soil mechanic model tests and to predict collision events not covered by the hydraulic model tests.

6.2 Hydraulic Model Set-up

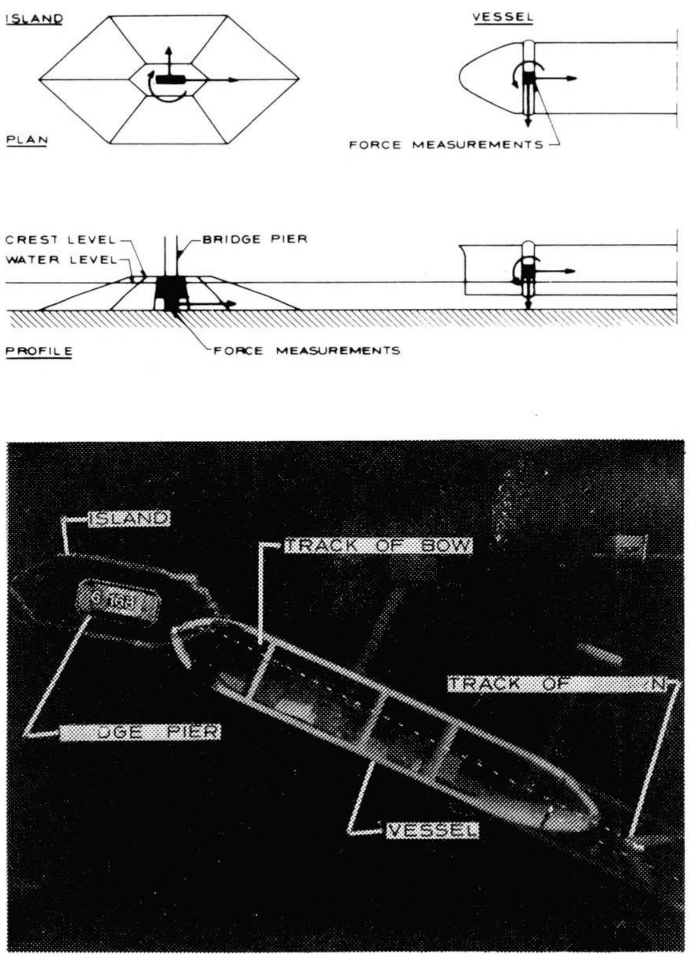

Fig. No. 5 Hydraulic Model Set-up.

Most tests were performed with a 250,000 DWT and a 150,000 DWT tanker. Some were carried out with a 50,000 DWT container ship. Altogether approximately 500 tests were performed. The model length scales were 1:94 and 1:79. Froude-scaling was applicable. The rubble mound slopes and islands consisted of uniform sharply crushed stones, corresponding to 400 kg stones in nature. The slopes were in all tests 1:1.5 and the berms were horizontal.

The tracks of the vessels were registered by a camera which was mounted above the protection structure. Flashing lights on the bow and the stern clearly indicated the tracks and the velocities of these parts of the vessel, see Fig. No. 5.

Further, the speed was measured by a photo cell right before the collision.

The vessel could move freely during the collision.

The model ship bow was cut off and reconnected to the hull through dynamometers. In this way three force components and two moment components were measured simultaneously during the collision. The bridge pier was fastened to the floor of the laboratory through a dynamometer, too. Two force components and one moment component were measured simultaneously.

6.3 Collisions with Rubble Mound Slopes

From the first series of model tests the influence of approach angle and shape of ship bow is summarized in Fig. No. 6.

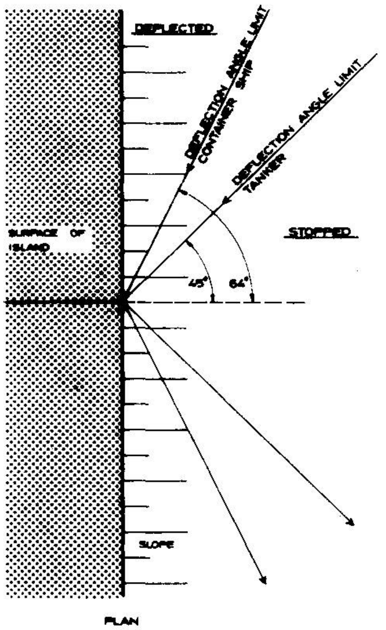

Fig. No. 6 Deflective Characteristics of Rubble Mound Slopes.

In the case of a head-on collision the vessel penetrates into the protection slope until it is ultimately stopped. An obliquely incoming vessel may be deflected by the protection structure and continue with decreased speed. The limiting approach angle determining the favourable deflecting behaviour depends on the shape of the ship bow. The long narrow bow of a container ship almost steers the ship into the protection slope from where it will only escape for courses which are rather parallel to the structure. The tanker has a rounded bow and is deflected even for approach angles of 45° with the alignment of the structure.

The soil mechanic tests were carried out for tanker bows only as they were considered the more relevant for the Great Belt Bridge Project. In the following all results refer to vessels with tanker bow shapes. From the soil mechanic tests the following formulation was adopted for modelling the contact force for all contact areas of the vessel having a velocity component towards the structure.

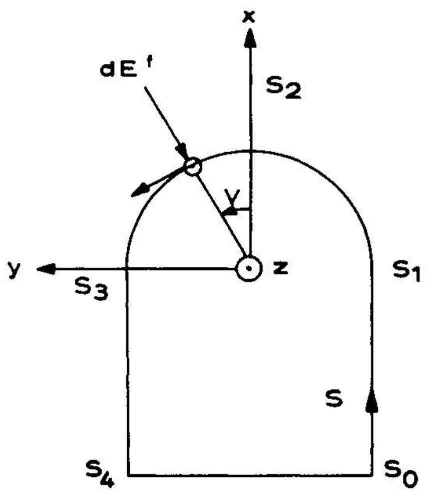

$$F_x = \int_{s1}^{s3} (\cos v + \mu \sin^3 v)\, dE^f$$

$$F_y = \int_{s1}^{s2} (\sin v + \mu \cos v \sin^2 v)\, dE^f + \int_{s2}^{s3} (\sin v - \mu \cos v \sin^2 v)\, dE^f$$

$$F_z = \int_{s1}^{s3} \mu \cos^2 v\, dE^f$$

Fig. No. 7 Definition Sketch. Contact Forces.

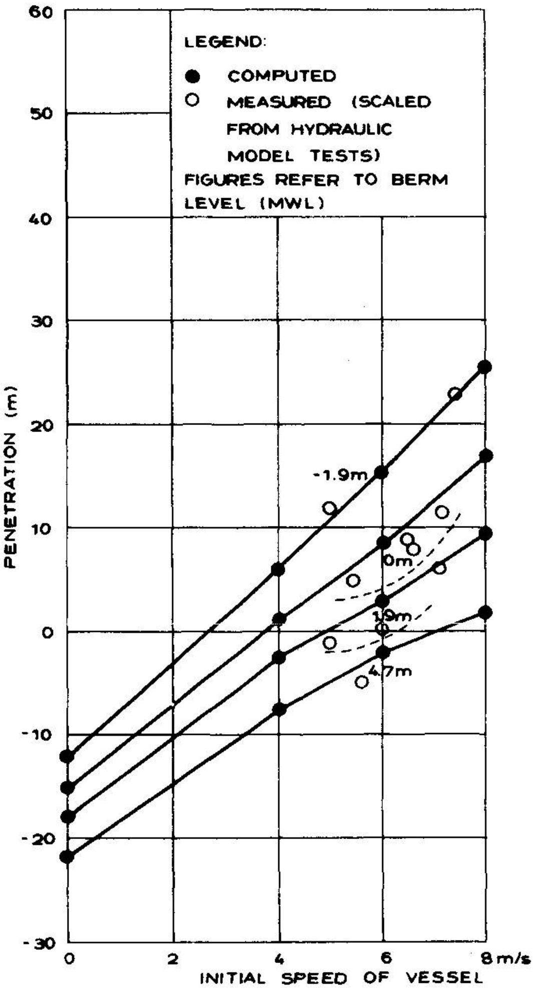

A semi-analytical expression for the force component dE^{I} was derived by the Danish Geotechnical Institute (1978). This expression took into account the vertical depth of penetration, the effect of the berm on earth pressure in the sloping part of the structure, the additional pressure from displaced material, and the reduction in contact force near corners of the protection island.

The outer force and moment was computed by integrating the above expression along the vessel's bow.

Fig. No. 8 shows computed and measured penetrations for a 250,000 DWT tanker with a draught of 10 m, which collides head-on with a rubble mound slope (1:1.5). The influence of different collision speeds and berm levels was examined. The penetration is measured from the intersection between the slope and the berm. For vessel speeds up to 8 m/s good agreement between measured and computed penetrations was obtained.

Fig. No. 8 Measured and Computed Penetrations for a 250,000 DWT Tanker, Draught 10 m. Slope (1:1.5).

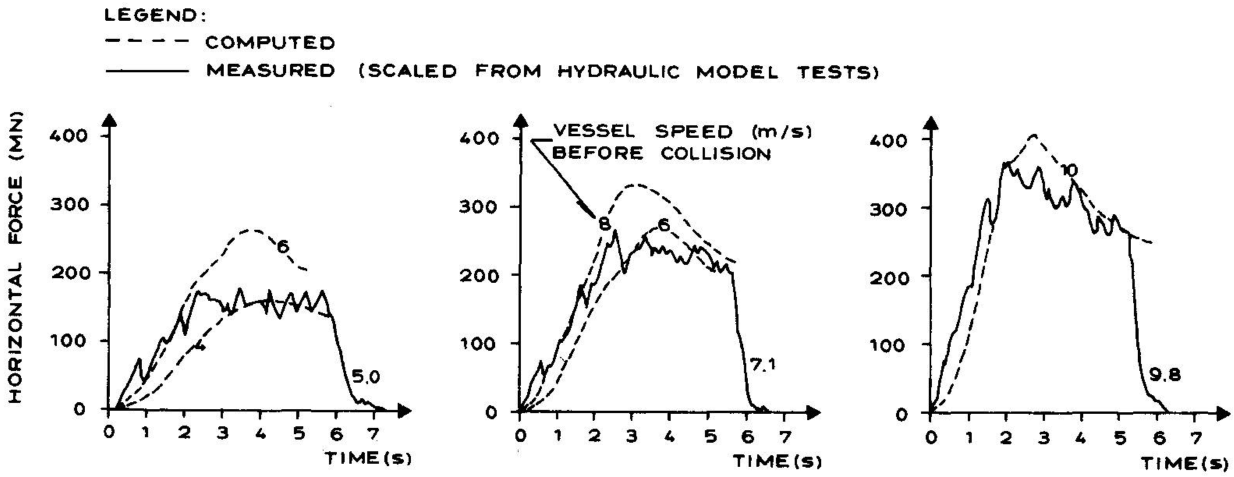

Fig. No. 9 Computed and Measured Collision Forces for a 250.000 DWT Tanker, Draught 10 m. Berm Level 1.9 m (MWL).

Fig. No. 9 shows a comparison between computed and measured horizontal collision forces in the case with a berm level of 1.9 m above the mean water level (MWL). It is seen that close agreement has been obtained for the entire collision event for a wide range of collision speeds. As discussed in Chapter 5 these horizontal force-time diagrams for head-on collisions directly show how the initial momentum of the vessel is brought to zero, in these cases by a fairly constant force which is reached when most of the ship bow below the berm level is involved in the collision.

Fig. No. 10 shows comparisons between measured and computed penetration distances for obliquely incoming vessels, again for a 250,000 DWT tanker with a draught of 10 m.

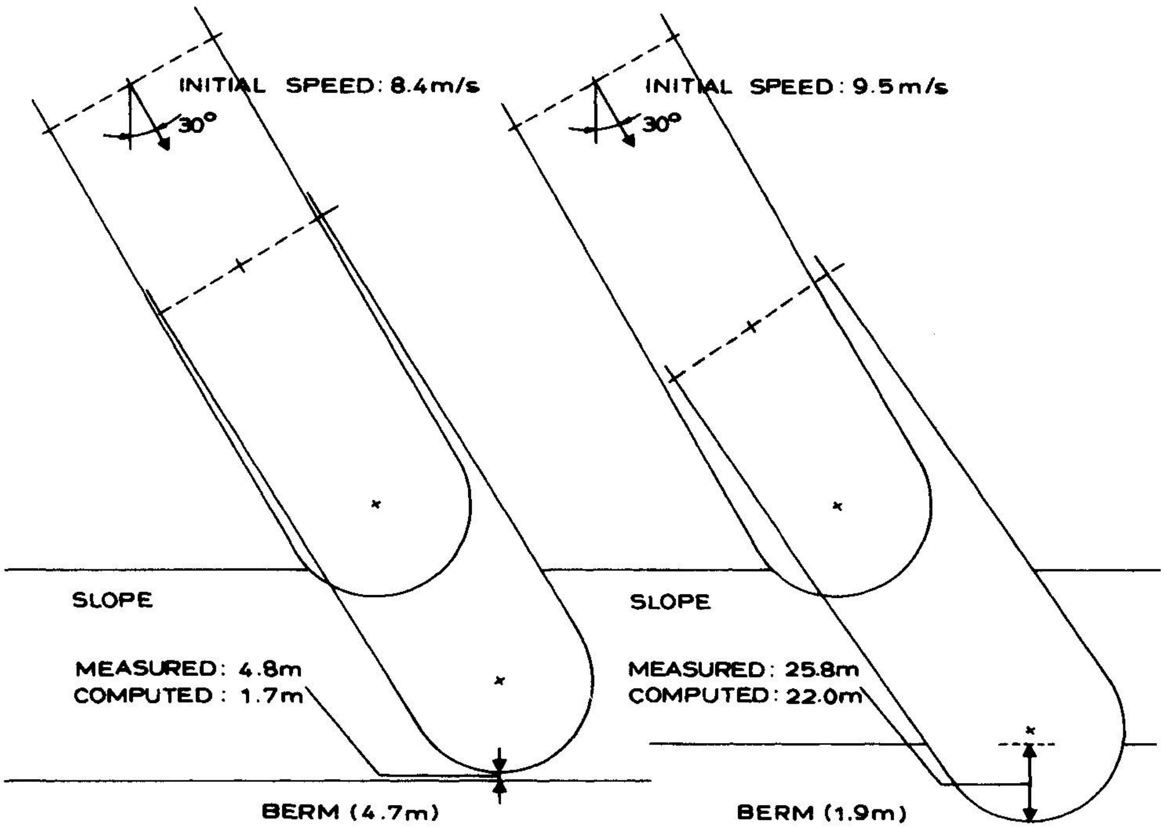

Fig.No. 10 Measured and Computed Penetrations for an Obliquely Incoming 250,000 DWT Tanker, Draught 10 m.

6.4 Collision with Rubble Mound Islands

Fig. No. 11 illustrates that also the deflecting characteristics of a protective island can be computed in close agreement with measurements. This supports the idea of modelling contact forces between vessels and structures in rather detail as it was done here with a complex distribution of the contact pressure along the ship bow.

It is also seen from Fig. No. 11 (and documented in detail by the hydraulic model tests) that vessels which approach the protection island from the approach angle here shown are almost inevitably deflected.

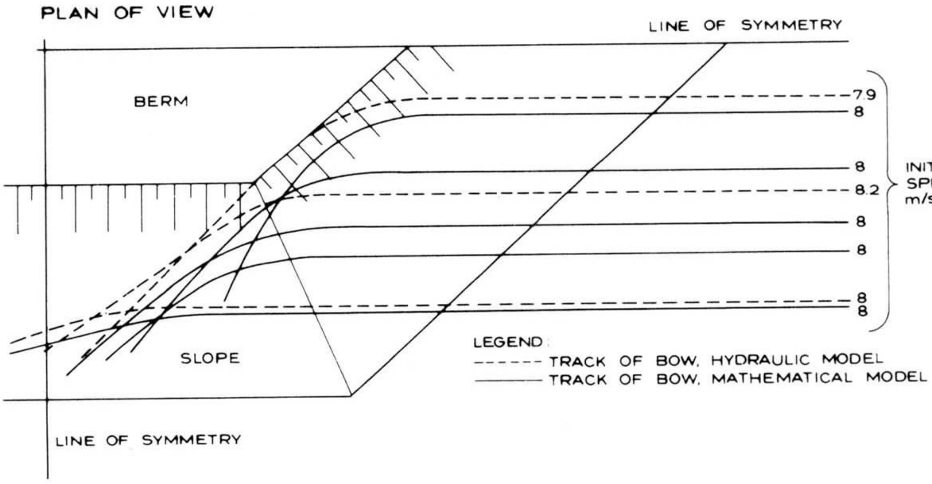

Fig. No. 11 Measured and Computed Bow Tracks for a 250,000 DWT Tanker, Draught 10 m.

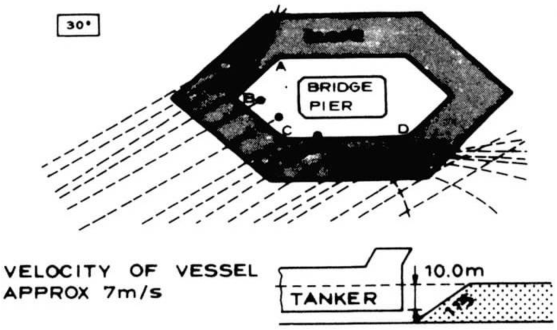

Fig. No. 12 shows that the important deflective characteristics are maintained for vessels approaching under a more infavourable approach angle.

Fig. No. 12 Bow Tracks for 250,000 DWT Tanker, Draught 10 m, Colliding with a Protection Island.

Fig. No. 13 summarizes the significance of having structures with optimal deflective characteristics. Not only the horizontal collision forces between the vessel and the structure decreases rapidly when the vessel is deflected, but the horizontal force ultimately transferred to the bridge pier is further reduced.

Consequently, the probabability of occurence of a given impact force can be significantly reduced by protective rubble mound structures. Such protective structures can therefore be considered a realistic type of solution for reaching an acceptable risk level for structures exposed to high-energy collisions.

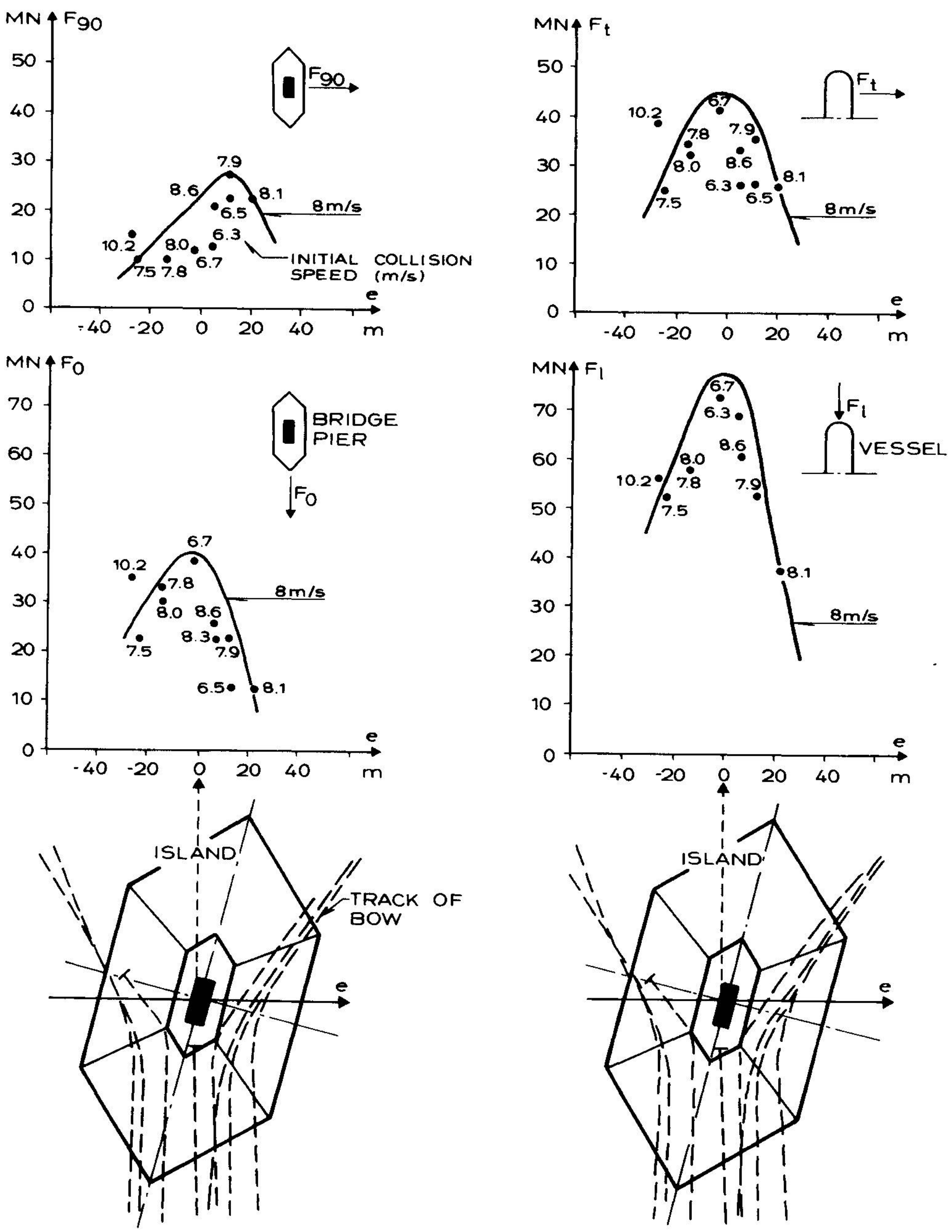

Fig. No. 13 Measured Forces in Bridge Pier and Vessel for 150,000 DWT Tanker, Draught 10 m, Colliding with Rubble Mound Island.

6.5 Other Applications

It could be mentioned that the computational procedure outlined above has been applied for the evaluation of penetration depths from ships grounding in the Danish Belts and that the results so obtained were used for deciding on trenching depths and spacing between marine gas pipelines, presently being laid in the Danish Belts.

7. DEFORMABLE VESSEL AGAINST DEFORMABLE STRUCTURE

The more general formulation of the collision problem operates with the load-deformation curves for both vessel and structure. Such formulations exist for two colliding vessels and e.g. also for low-energy collisions between a swaying vessel and an offshore platform, Petersen and Pedersen (1980).

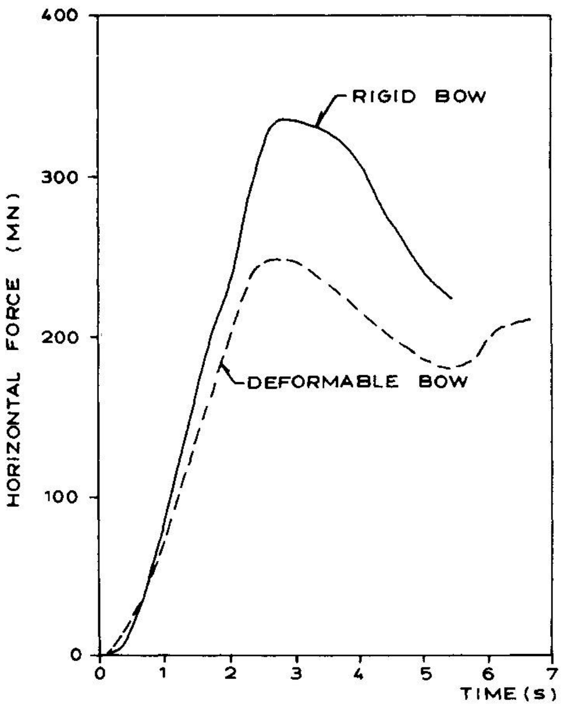

Fig. No. 14 Comparison between computed Horizontal Forces for Rigid and Deformable Ship Bows

For high-energy collisions between a vessel and a rubble mound slope, Fuchs et al (1978) combined the assumptions presented in Chapter 5 and 6 for the vessel and the protective structure, respectively. This leads to a simplified description in which the vessel initially penetrates as a rigid body, but at a certain depth below the structure's surface, the contact pressure exceeds the strength of the vessel which in turn is deformed rather than the structure. This formulation therefore leads to smaller collision forces than those presented in Chapter 6. This is demonstrated in Fig. No. 14 which shows the computed horizontal collision forces for a head-on collision between a 250,000 dwt tanker, draught 10 m, and a rubble mound structure with a berm level of 1.9 m (MWL). The vessel was assumed to be rigid in one case and to be deformable with a contact force/area ratio of $5\ 10^5$ N/m^2 in the second case.

On one hand, the deformation of the vessel leads to smaller collision forces than those measured and computed for the rigid vessel. On the other hand, the upper part of the ship's bow will move a greater distance over the berm and thereby increase the probability of direct contact between the vessel and the main structure.

8. CONCLUSIONS

The consequences of a collision between a vessel and a protective structure are determined by many parameters such as the speed, course, size, bow shape and hull stiffness of the vessel and the strength and geometrical shape of the protective structure.

These parameters can all be taken into account by applying a deterministic description which is based on classical mechanical principles.

In case existing knowledge on some of the subprocesses of a collision is insufficient, model tests can be planned and interpreted with great economy of effort when the results are to be integrated with a deterministic formulation into one single body of knowledge. In this paper this point is illustrated in detail by results obtained for the planning of the now postponed Great Belt Bridge (Denmark).

9. ACKNOWLEDGEMENTS

The authors wish to thank Statsbroen Store Baelt (SSB) for permission to publish this paper and to use results from other consultants of SSB, notably Storebæltsgruppen, consulting engineers and planners, the Ship Research Laboratory, The Danish Geotechnical Institute and the Danish Hydraulic Institute.

10. REFERENCES

ANDO, N. and ARITA, K., A Study on the Strength of Double-Hull Structures in Collision, (in Japanese), Trans. Soc. of Naval Arch. of Japan, 139, 147-156, 1976.

ARITA, M., ANDO, N., ARITA, K., Study on the Structural Strength of Ships in Collision, Conference on Fracture Mechanics and Technology, Hong Kong, 1977.

DANISH GEOTECHNICAL INSTITUTE, Geotekniske Modelforsøg. Rapport nr. 2 med bilag 37-54, (in Danish), 1978.

FUCHS, J. U., HAVNØ, K., TRYDE, P., BRINK-KJÆR, O., Skibsstød mod faste konstruktioner og sandøer, (in Danish), Institute of Hydrodynamics and Hydraulic Engineering, Technical University of Denmark, 1978.

IWAI, A., NAGASAWA, H., ODA, K., SHOJI, K., Ship-bridge pier protective systems, proc. Coastal Engineering Conference, 1980.

JONES, N., A litterature survey on the collision and grounding protection of ships, U. S. Coast Guard Headquarters, Washington D.C., 1979.

MINORSKY, V. U., An Analysis of Ship Collisions with Reference to Protection of Nuclear Power Plants, J. Ship Research, 3, 1-4, 1974.

MOTORA, S., FUJINO, M., SUGIURA, M., SUGITA, M., Equivalent Added Mass of Ships in Collisions, Selected Papers from the Journal of the Society of Naval Architects of Japan, 7, pp. 138-148, 1971.

NAGASAWA, H., ARITA,K., TANI, M., OKA,S., A Study on the Collapse of Ship Structure in Collision with Bridge Piers (in Japanese), Trans. Soc. of Naval Arch. of Japan, 142, 345-354, 1977.

OLNHAUSEN, M. VON, Påsegling av Bropelare, Teknisk Tidsskrift, (in Swedish), Hæfte 17, 1966.

PETERSEN, M. J., Dynamics of Ship Collisions, DACAMM, Report No. 185, Technical University of Denmark, July 1980.

PETERSEN, M. J., and PEDERSEN, P. T., Collisions between Ships and Offshore Platforms, proc. Offshore Technology Conference, 1981.

RECKLING, K. A., Beitrag der Elasto- und Plastomechanic zur Untersuchung von Shiffskollisionen, (in German), Jahrbuch der Schiffbautechnischen Gesellschaft, 70, 443-464, 1976.

RECKLING, K. A., On the Collision Protection of Ships, Int. Symp on Practical Design in Shipbuilding, Soc. of Naval Architects of Japan, Tokyo, 129-134, 1977.

SALVESEN, N., TUCK, E. O., FALTINSEN, O., Ship Motions and Sea Loads, S.N.A.M.E. Transactions, 1970.

WOISIN, G., Schiffbauliche Forschungsarbeiten für die Sicherheit Kernenergi-getriebener Handelsshiffe, (in German), Jahrbuch der Schiffbautechnischen Gesellschaft, 65, 225-263, 1971.